View Article Online / Journal Homepage / Table of Contents for this issue
Dynamic Article Links

CrystEngComm

Cite this: *CrystEngComm*, 2012, **14**, 379

www.rsc.org/crystengcomm

COMMUNICATION

3D → 3D interpenetrated and 2D → 3D polycatenated Ag(I) networks constructed from 1,4-bis(2-methylimidazol-1-ylmethyl)benzene and dicarboxylates†

Fu-Jing Liu,‡[a] Di Sun,‡*[b] Hong-Jun Hao,[a] Rong-Bin Huang*[a] and Lan-Sun Zheng[a]

Received 12th October 2011, Accepted 31st October 2011
DOI: 10.1039/c1ce06356a

Published on 16 November 2011. Downloaded by Xiamen University on 12/07/2015 14:01:59.

Two novel entangled Ag(I) metal–organic frameworks (MOFs), namely $[Ag_2(bmimb)_{1.5}(pzdc)\cdot 3H_2O]_n$ (1) and $[Ag(bmimb)(mac)_{0.5}\cdot 0.5H_2O]_n$ (2) (bmimb = 1,4-bis(2-methylimidazol-1-ylmethyl)benzene, H_2pzdc = pyrazine-2,3-dicarboxylic acid, H_2mac = L-malic acid), exhibit 3D → 3D interpenetrated and 2D → 3D polycatenated motifs, respectively, which were modulated by auxiliary dicarboxylates. Moreover, the UV-Vis spectra, thermal stabilities and photoluminescent properties were also discussed.

Entangled coordination networks have provided a long-standing fascination for crystal engineers not only due to their intrinsic aesthetic appeal and potential properties, but also for their intricate molecular architectures and topologies.[1] Numerous appealing entangled networks have been constructed and discussed in excellent reviews by Robson, Batten, Ciani, Proserpio and their co-workers.[2] Recently, some novel types of entangled networks including polyrotaxane, polycatenane, polyknotting and Borromean ring have seen growth accompanying the advance of crystal engineering.[3] Among the entangled systems, polycatenane is an especially interesting type which is characterized by the interlocked rings and each individual ring is locked only with the surrounding ones but not with all the others.[4] Anyway, MOFs showing the polycatenane character are an interesting challenge and remain largely unexplored. These are still quite rare, therefore, further research is necessary to enrich and develop this field. On the other hand, using classical synthetic routes and methods to achieve polycatenane has been proved to be a huge challenge for synthetic chemists, however, the 'one-pot' self-assembly has found an important niche in this field.

As an ongoing investigation on synthesis of novel entangled networks,[5] we are currently investigating the use of the flexible ligand 1,4-bis(2-methylimidazol-1-ylmethyl)benzene (bmimb) to construct novel architectures, since this spacer may give novel entangled networks such as $\{[Ag_2(bmimb)_3](BF_4)_2\}_n$, an elegant Borromean honeycomb sheet supported by argentophilic interactions.[6] As indicated by a CSD (Cambridge Structure Database) survey with the help of ConQuest version 1.3,[7] only five Ag/bmimb complexes were documented in four papers,[6,8] while an Ag/bmimb complex incorporating an auxiliary ligand has not been disclosed yet. Given the above challenges and considering our previous work on the assembly of Ag(I) complexes using the mixed-ligand strategy,[9] herein, we synthesized and characterized two novel entangled Ag(I) networks, $[Ag_2(bmimb)_{1.5}(pzdc)\cdot 3H_2O]_n$ (**1**) and $[Ag(bmimb)(mac)_{0.5}\cdot 0.5H_2O]_n$ (**2**) (bmimb = 1,4-bis(2-methylimidazol-1-ylmethyl)benzene, H_2pzdc = pyrazine-2,3-dicarboxylic acid, H_2mac = L-malic acid) (Scheme 1), exhibiting unprecedented 3D → 3D interpenetrated and 2D → 3D polycatenated motifs, respectively.

Ultrasonic treatment of equimolar amounts of Ag_2O, bmimb and different dicarboxylates in methanol–DMF (5 mL, v/v = 3 : 2) with 2 mL ammonia gave the crystals of complexes **1** and **2** by slow evaporation (see ESI†). The compositions of **1** and **2** were further deduced from X-ray single crystal diffraction, elemental analysis, and IR spectra. The solid FT-IR spectra (Fig. S1, ESI†) of complexes **1** and **2** show the characteristic bands for solvent water molecules and

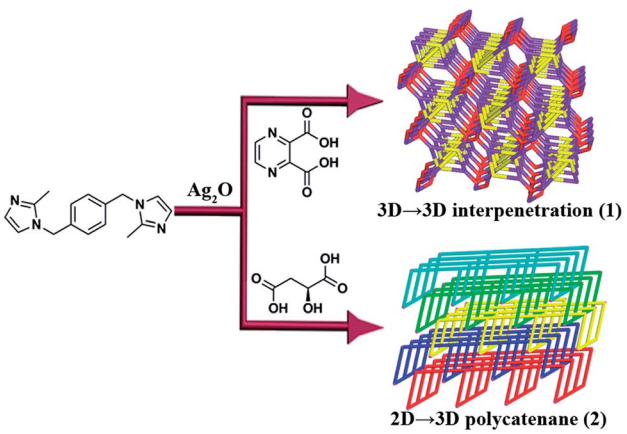

Scheme 1 Synthetic procedures for **1** and **2**.

[a]*State Key Laboratory of Physical Chemistry of Solid Surface and Department of Chemistry, College of Chemistry and Chemical Engineering, Xiamen University, Xiamen, China. E-mail: rbhuang@xmu.edu.cn; Fax: +86-592-2183047*
[b]*School of Chemistry and Chemical Engineering, Shandong University, Jinan, Shandong, 250100, China. E-mail: dsun@sdu.edu.cn; Fax: +86-531-88364218*

† Electronic supplementary information (ESI) available: Synthetic and crystallographic details, additional measurements, figures and tables. CCDC reference numbers 845056 and 845057. For ESI and crystallographic data in CIF or other electronic format see DOI: 10.1039/c1ce06356a

‡ These authors contributed equally to this work.

View Article Online

Published on 16 November 2011. Downloaded by Xiamen University on 12/07/2015 14:01:59.

deprotonated carboxyl groups. The powder X-ray diffraction (PXRD) patterns of **1** and **2** are coincident with the simulated pattern derived from the X-ray single crystal data, implying that the bulk sample is the same as the single crystal (Fig. S2, ESI†).

X-Ray single-crystal diffraction analysis§ reveals that **1** is a unique 3D → 3D two-fold interpenetrated motif. It crystallizes in the monoclinic *C*2/*c* space group with an asymmetric unit that contains two Ag(I) ions, one and a half bmimb ligands, one pzdc anion, and three lattice water molecules. As depicted in Fig. 1a, the Ag1 and Ag2 are located in a distorted square pyramidal ($\tau_5 = 0.11$)[10a] and tetrahedral ($\tau_4 = 0.65$)[10b] geometry, respectively. The coordination environment of Ag1 is completed by two O atoms from two different pzdc ligands and three N atoms from two different pzdc and one bmimb ligands, while Ag2 is coordinated by two O atoms from the same pzdc and two N atoms from two different bmimb ligands. The flexible bmimb ligands in **1** show two different conformations, *anti* and *syn* (Scheme S1†), which are responsible for the formation of rodlike [Ag_2(bmimb)] segments and [Ag_2(bmimb)$_2$] loops, respectively. The stereochemical relationship between the [Ag_2(bmimb)] rod and [Ag_2(bmimb)$_2$] loop is the former passing through the latter (Fig. S3†), and they shared the same crystallographic inversion center. The *anti*-bmimb and μ_3-(η_2–N,O), (η_2–N′,O″), (η_2–O′,O″)-pzdc ligands link Ag(I) ions to generate a 2D sheet. From a topological viewpoint, the sheet can be considered as a (6,3) net, which is further supported by [Ag_2(bmimb)$_2$] loops to form a single 3D framework (Fig. S4†).

The most fascinating feature of **1** is depicted in Fig. 1b and c, two rodlike [Ag_2(bmimb)] segments incorporate four trigonal [Ag_3(pzdc)] segments to form a dumbbell-like 46-membered macrocycle which is large enough to simultaneously lock two 26-membered macrocycles (Fig. S5†), generating an interlocked subunit. The entanglement of single networks in the crystal structure of **1** results in the complicated 3D framework with the interpenetration character (Fig. 1d). Based on above structural analysis, the overall architecture of **1** can be seen as a two-fold 3D → 3D interpenetrated network (Fig. 1e). Although some 1D → 1D and 2D → 2D interpenetrated networks have been reported in the literature,[11] 3D → 3D interpenetrated networks are, at present, still rare. The successful self-assembly of **1** not only presents a fascinating 3D → 3D interpenetrated example but also opens up new perspectives to the novel entangled networks.

When the H_2pzdc was replaced by H_2mac, we obtained complex **2** as a 2D → 3D polycatenated structure. X-Ray single-crystal diffraction analysis§ reveals that the asymmetric unit of **2** contains one Ag(I) ion, one bmimb with *anti*-conformation, half mac anion, and half lattice water molecules (Fig. 2a). The Ag1 adopts a T-shaped coordination configuration with two N atoms of bmimb in the horizontal direction. The coordination environment is completed by one O atom of mac in the axial direction forming a T-shaped unit. As shown in Fig. 2b, the Ag(I) ions are ligated by bmimb to form infinite 1D [Ag(bmimb)]$_n$ chains which are prolongated along two directions forming a torsion angle of 51.86°. A pair of related [Ag(bmimb)]$_n$ chains are interlinked by a mac pillar to form bilayer galleries. The width and thickness of the galleries are determined by the length of bmimb (13.61 Å) and mac (8.98 Å), respectively. The Ag(I) ion serves as a 3-connected node in **2**, then the bilayer can be simplified to a 3-connected uninodal net with {8^2.10} topology.[12]

In **2**, the bilayer contains both long and short mixed ligands, which displays a complicated entanglement between the adjacent bilayers (Fig. 2c). The overall structure of **2** belongs to a 3D framework built from 2D → 3D polycatenation of 'thick' bilayers, that is, each bilayer is catenated by two adjacent (one upper and one lower) equivalent ones. The most related example is {[Ag(bpe)(bpdc$_{0.5}$)]·H_2O}$_n$ (**3**, bpe = 1,2-bis(4-pyridyl)ethane, bpd = 4,4′-biphenyldicarboxylate), which

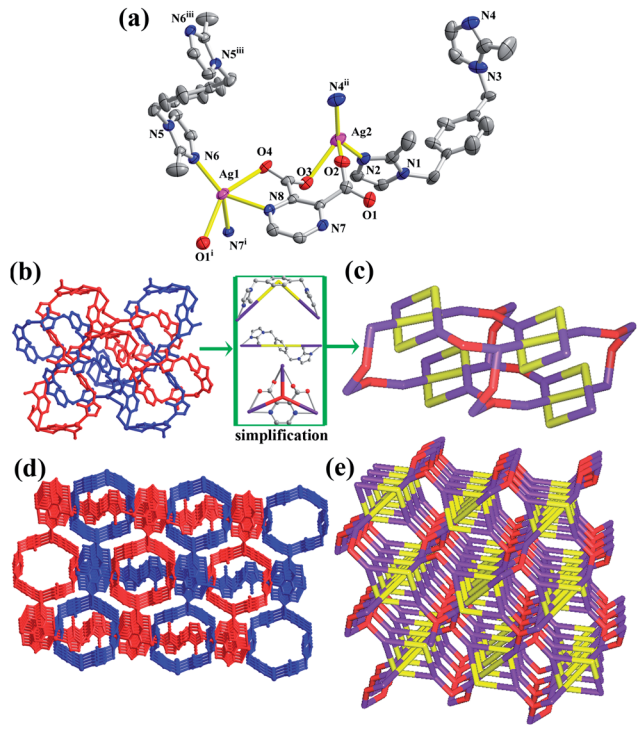

Fig. 1 Crystal structure of **1**. Thermal ellipsoid (50%) plot of **1** showing the coordination environment of Ag(I) ions (a). The ball and stick view (b) and simplified (c) interlocked 26- and 46-membered macrocycles. Schematic drawing of the 3D interpenetrated framework (d) and its simplified equivalence (e). (Symmetry codes: (i) $-x + 3/2$, $y + 1/2$, $-z + 3/2$; (ii) $-x + 1$, $-y + 1$, $-z + 2$; (iii) $-x + 1$, $-y + 1$, $-z + 1$.)

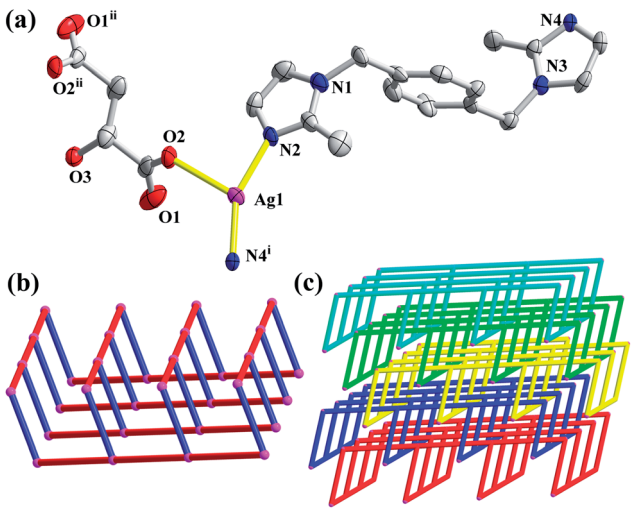

Fig. 2 Crystal structure of **2**. Thermal ellipsoid (50%) plot of **2** showing the coordination environment of Ag(I) ion (a). The ball and stick view of molecular bilayer motif of **2**, constructed by mac (blue) and bmimb (red) ligands (b). Schematic drawing of the 2D → 3D polycatenated framework (c). (Symmetry codes: (i) $x - 1/2$, $y - 1/2$, $z - 1$; (ii) $1 - x$, y, $1 - z$.)

This journal is © The Royal Society of Chemistry 2012

View Article Online

Published on 16 November 2011. Downloaded by Xiamen University on 12/07/2015 14:01:59.

was firstly reported by Wu and co-workers,[13] then the unusual and puzzling topology of **3** was elaborated by Ciani *et al.*[2e] The polycatenation mode of **2** is clearly dissimilar from **3**, which consisted of two groups of catenated bilayers with each 2D bilayers associated just with the two nearest neighbors belonging to the identical group. Notably, the relationship between two different groups can be described as the simple interdigitation instead of polycatenation. The higher degree of entanglement of **3** may be due to the fact that the bilayer constructed by two linkers with different lengths (13.72 Å for bpe and 16.36 Å for bpdc) has a larger void for interdigitation than the bilayer in **2** comprising one long and one short linker (13.61 Å for bmimb and 8.98 Å for mac).

The thermogravimetric (TG) curves (Fig. 3) were measured in N_2 atmosphere. For **1** and **2**, a weight loss of 6.94% (calcd: 6.47%) and 2.55% (calcd: 2.01%) at 60–130 and 80–170 °C, respectively, corresponds to complete dehydration. The decomposition of the anhydrous components of **1** and **2** starts at about 155 and 175 °C, respectively, accompanying the release of organic ligands.

Powder X-ray diffraction (PXRD) has been used to check the phase purity of the bulky samples in the solid state (Fig. S6†). For complexes **1** and **2**, the peak positions of simulated and experimental patterns are in good agreement with each other, demonstrating the phase purity of the product. The dissimilarities in intensity may be due to the preferred orientation of the crystalline powder samples. The PXRD of dehydrated samples **1′** and **2′** (heating the samples **1** and **2** to 150 °C in a vacuum) indicates that the host entangled frameworks can be retained as compared to those of as-prepared samples (Fig. S6†).

The absorption spectra of **1** and **2** are shown in Fig. S7†, both complexes show the high-energy absorption bands in the range of 200–400 nm (285, 343 nm for **1** and 235, 266 nm for **2**) which are ascribed to the intraligand $\pi \rightarrow \pi^*$ transitions of the bmimb moiety. As shown in Fig. 4, the free ligand bmimb displays photoluminescence with the emission maximum at 491 nm ($\lambda_{ex} = 350$ nm). It can be presumed that this peak originates from the $\pi \rightarrow \pi^*$ transition. The emission bands of dicarboxylate ligands can be assigned to the $n \rightarrow \pi^*$ transition.[14] Since the emission of the dicarboxylate ligands resulting from the $n \rightarrow \pi^*$ transition is very weak compared to that from the $\pi \rightarrow \pi^*$ transition of the bmimb ligand, the dicarboxylate ligands almost have no contribution to the emissions of **1–2**.[5a] Compared with the emission of bmimb, the main emissive peaks of **1** and **2** are located in blue-shifted positions 473 and 426 nm ($\lambda_{ex} = 350$ nm), respectively. These emissions probably can be assigned to the Ag(I)-perturbed intraligand (IL) $\pi \rightarrow \pi^*$ transition of the bmimb ligand. Interestingly, the emissions of anhydrous **1′** and **2′** show red shifts of 3 and 50 nm, respectively, compared to those of **1** and **2**. These could be explained by the existence of hydrogen bonds between the lattice water molecules and the frameworks in **1** and **2**.[15]

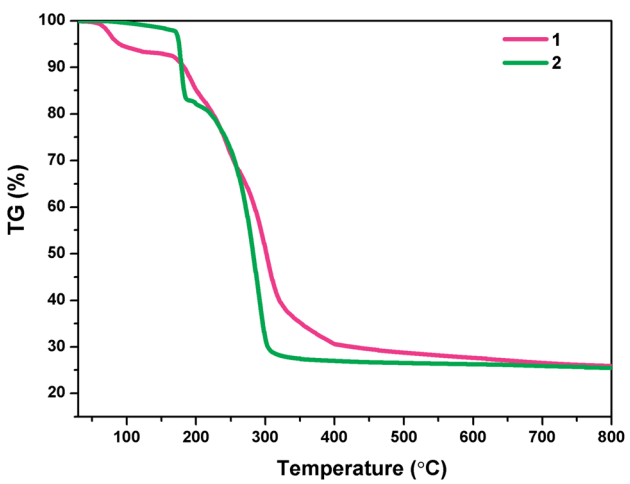

Fig. 3 The TGA curves of **1** and **2**.

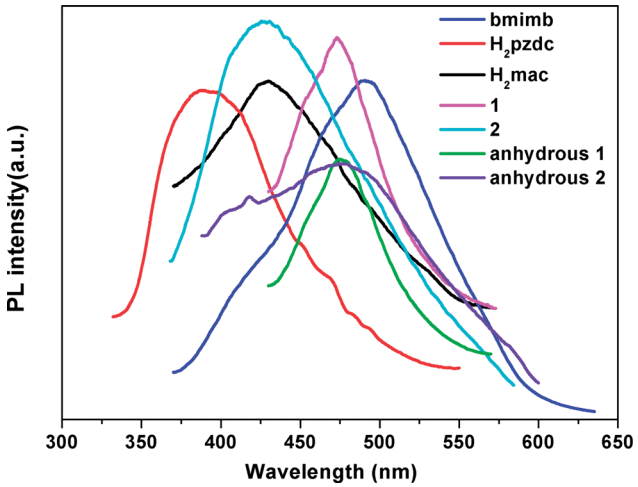

Fig. 4 The photoluminescence spectra of free ligands, **1**, **2** and dehydrated **1** and **2**.

In summary, we have presented two novel entangled Ag(I) mixed-ligand MOFs, which exhibit unusual 3D → 3D interpenetrated and 2D → 3D polycatenated motifs, respectively. Moreover, the thermal stabilities, UV absorption as well as emissive behaviors were also discussed.

This work was financially supported by the National Natural Science Foundation of China (no. 21021061 and 21071118), 973 Project (Grant 2007CB815301) from MSTC, and Independent Innovation Foundation of Shandong University (2011GN030).

Notes and references

§ Crystal data for **1**: $C_{30}H_{33}Ag_2N_8O_7$, $M = 833.38$ g mol^{-1}, monoclinic, space group $C2/c$, $Z = 8$, $a = 25.317(12)$, $b = 9.877(5)$, $c = 26.864(12)$ Å, $\beta = 104.382(16)°$, $V = 6507(5)$ Å^3, $D_c = 1.701$ g cm^{-3}, $R_1 = 0.0671$, w$R_2 = 0.1698$, $S = 1.120$. Crystal data for **2**: $C_{36}H_{41}Ag_2N_8O_6$, $M = 897.51$ g mol^{-1}, monoclinic, space group $C2$, $Z = 2$, $a = 18.193(8)$, $b = 11.273(5)$, $c = 8.606(4)$ Å, $\beta = 91.271(8)°$, $V = 1764.6(13)$ Å^3, $D_c = 1.689$ g cm^{-3}, $R_1 = 0.0543$, w$R_2 = 0.1262$, $S = 1.154$.

1 (*a*) K. M. Park, D. Whang, E. Lee, J. Heo and K. Kim, *Chem.–Eur. J.*, 2002, **8**, 498; (*b*) V. Niel, A. L. Thompson, M. C. Muñoz, A. Galet, A. E. Goeta and J. A. Real, *Angew. Chem., Int. Ed.*, 2003, **42**, 3760; (*c*) J. A. Aitken and M. G. Kanatzidis, *J. Am. Chem. Soc.*, 2004, **126**, 11780; (*d*) L. Q. Ma and W. B. Lin, *Angew. Chem., Int. Ed.*, 2009, **48**, 3637; (*e*) Y. Gong, Y. C. Zhou, T. F. Liu, J. Lu, D. M. Proserpio and R. Cao, *Chem. Commun.*, 2011, **47**, 5982; (*f*) R. L. LaDuca, *Coord. Chem. Rev.*, 2009, **253**, 1759; (*g*) X. F. Kuang, X. Y. Wu, R. M. Yu, J. P. Donahue, J. S. Huang and C. Z. Lu, *Nat. Chem.*, 2010, **2**, 461; (*h*) O. Shekhah, H. Wang, M. Paradinas, C. Ocal, B. Schupbach, A. Terfort, D. Zacher, R. A. Fischer and C. Woll, *Nat. Mater.*, 2009, **8**, 481; (*i*) A. S. Degtyarenko, P. V. Solntsev, H. Krautscheid, E. B. Rusanov, A. N. Chernega and K. V. Domasevitch, *New J. Chem.*, 2008, **32**, 1910; (*j*) H. He, D. Yuan, H. Ma, D. Sun, G. Zhang and

View Article Online

Published on 16 November 2011. Downloaded by Xiamen University on 12/07/2015 14:01:59.

H.-C. Zhou, *Inorg. Chem.*, 2010, **49**, 7605; (*k*) X. Zhao, H. He, T. Hu, F. Dai and D. Sun, *Inorg. Chem.*, 2009, **48**, 8057.

2 (*a*) V. A. Blatov, L. Carlucci, G. Ciani and D. M. Proserpio, *CrystEngComm*, 2004, **6**, 378; (*b*) I. A. Baburin, V. A. Blatov, L. Carlucci, G. Ciani and D. M. Proserpio, *CrystEngComm*, 2008, **10**, 1822; (*c*) S. R. Batten and R. Robson, *Angew. Chem., Int. Ed.*, 1998, **37**, 1460; (*d*) S. R. Batten, *CrystEngComm*, 2001, **3**, 67; (*e*) L. Carlucci, G. Ciani and D. M. Proserpio, *Coord. Chem. Rev.*, 2003, **246**, 247.

3 (*a*) X.-L. Wang, C. Qin, E.-B. Wang, Y.-G. Li, Z.-M. Su, L. Xu and L. Carlucci, *Angew. Chem., Int. Ed.*, 2005, **44**, 5824; (*b*) Y.-Q. Lan, S.-L. Li, J.-S. Qin, D.-Y. Du, X.-L. Wang, Z.-M. Su and Q. Fu, *Inorg. Chem.*, 2008, **47**, 10600; (*c*) L.-F. Ma, Y.-Y. Wang, J.-Q. Liu, G.-P. Yang, M. Du and L.-Y. Wang, *CrystEngComm*, 2009, **11**, 1800.

4 L. Carlucci, G. Ciani and D. M. Proserpio, *CrystEngComm*, 2003, **5**, 269.

5 (*a*) D. Sun, N. Zhang, R.-B. Huang and L.-S. Zheng, *Cryst. Growth Des.*, 2010, **10**, 3699; (*b*) D. Sun, Q.-J. Xu, C.-Y. Ma, N. Zhang, R.-B. Huang and L.-S. Zheng, *CrystEngComm*, 2010, **12**, 4161.

6 L. Dobrzanska, H. G. Raubenheimer and L. J. Barbour, *Chem. Commun.*, 2005, 5050.

7 (*a*) F. H. Allen, *Acta Crystallogr., Sect. B: Struct. Sci.*, 2002, **58**, 380; (*b*) Cambridge Structure Database search, CSD Version 5.28 (November 2006) with 14 updates, (January 2007–Aug 2011).

8 (*a*) L. Dobrzanska, G. O. Lloyd, H. G. Raubenheimer and L. J. Barbour, *J. Am. Chem. Soc.*, 2005, **127**, 13134; (*b*) L. Dobrzanska and G. O. Lloyd, *Acta Crystallogr., Sect. E: Struct. Rep. Online*, 2006, **62**, m1638; (*c*) L. Dobrzanska, G. O. Lloyd, T. Jacobs, I. Rootman, C. L. Oliver, M. W. Bredenkamp and L. J. Barbour, *J. Mol. Struct.*, 2006, **796**, 107.

9 (*a*) D. Sun, G.-G. Luo, N. Zhang, R.-B. Huang and L.-S. Zheng, *Chem. Commun.*, 2011, **47**, 1461; (*b*) D. Sun, H.-R. Xu, C.-F. Yang, Z.-H. Wei, N. Zhang, R.-B. Huang and L.-S. Zheng, *Cryst. Growth Des.*, 2010, **10**, 4642; (*c*) D. Sun, Z. H. Wei, C. F. Yang, D. F. Wang, N. Zhang, R. B. Huang and L. S. Zheng, *CrystEngComm*, 2011, **13**, 1591; (*d*) D. Sun, D.-F. Wang, N. Zhang, F.-J. Liu, H.-J. Hao, R.-B. Huang and L.-S. Zheng, *Dalton Trans.*, 2011, **40**, 5677; (*e*) D. Sun, Y.-H. Li, H.-J. Hao, F.-J. Liu, Y. Zhao, R.-B. Huang and L.-S. Zheng, *CrystEngComm*, 2011, **13**, 6431; (*f*) D. Sun, Y.-H. Li, S.-T. Wu, H.-J. Hao, F.-J. Liu, R.-B. Huang and L.-S. Zheng, *CrystEngComm*, 2011, DOI: 10.1039/c1ce05672g; (*g*) D. Sun, H.-J. Hao, F.-J. Liu, H.-F. Su, R.-B. Huang and L.-S. Zheng, *CrystEngComm*, 2011, DOI: 10.1039/c1ce06089a.

10 (*a*) A. W. Addison, T. N. Rao, J. Reedijk, J. Van Rijn and G. C. Verschoor, *J. Chem. Soc., Dalton Trans.*, 1984, 1349; (*b*) L. Yang, D. R. Powell and R. P. Houser, *Dalton Trans.*, 2007, 955.

11 (*a*) M. A. Withersby, A. J. Blake, N. R. Champness, P. A. Cooke, P. Hubberstey and M. Schröder, *J. Am. Chem. Soc.*, 2000, **122**, 4044; (*b*) H. Wu, H. Y. Liu, Y. Y. Liu, J. Yang, B. Liu and J. F. Ma, *Chem. Commun.*, 2011, **47**, 1818; (*c*) B. F. Hoskins, R. Robson and D. A. Slizys, *Angew. Chem., Int. Ed. Engl.*, 1997, **36**, 2336.

12 V. A. Blatov, *TOPOS, A Multipurpose Crystallochemical Analysis with the Package*, Samara State University, Russia, 2004.

13 Z.-Y. Fu, X.-T. Wu, J.-C. Dai, S.-M. Hu and W.-X. Du, *New J. Chem.*, 2002, **26**, 978.

14 J. C. Dai, X. T. Wu, Z. Y. Fu, S. M. Hu, W. X. Du and C. P. Cui, *Chem. Commun.*, 2002, 12.

15 X.-L. Qi, R.-B. Lin, Q. Chen, J.-B. Lin, J.-P. Zhang and X.-M. Chen, *Chem. Sci.*, 2011, **2**, 2214.

 This journal is © The Royal Society of Chemistry 2012